Inorganic Chemistry
Article

Inorg. Chem. **2010**, *49*, 2827–2833 **2827**
DOI: 10.1021/ic902228h

Spinel to $CaFe_2O_4$ Transformation: Mechanism and Properties of β-$CdCr_2O_4$

Ángel M. Arévalo-López,*,† Antonio J. Dos santos-García,†,‡ Elizabeth Castillo-Martínez,†,§ Alejandro Durán,†,⊥ and Miguel Á. Alario-Franco†

†*Departamento de Química Inorgánica, Facultad de Químicas, Universidad Complutense de Madrid, 28040 Madrid, Spain,* ‡*Parque Científico y Tecnológico de Albacete, Instituto de Investigación en Energías Renovables, Fuel Cell Department, Universidad de Castilla—La Mancha, Paseo de la Innovación 1, 02006 Albacete, Spain, and* ⊥*Centro de Nanociencias y Nanotecnología, Universidad Nacional Autónoma de México, Apartado Postal 2681, C.P. 22800, Ensenada, B.C. México.* §*Present address: NanoTech Institue, University of Texas at Dallas, 800 Campbell Road BE26, Richardson, Texas 75252.*

Received November 11, 2009

The $CdCr_2O_4$ spinel transforms to a 10.6% denser new polymorph of the $CaFe_2O_4$-type structure at 10 GPa and 1100 °C. This new polymorph has a honeycomb-like structure because of double rutile-type chains formed by [Cr−O_6] edge-shared octehedra. This crystal structure is prone to be magnetically frustrated and presents low-dimensional antiferromagnetism at 25 K < *T* < 150 K, accompanied by more complex interactions as the temperature decreases. These transitions are evidenced by magnetic susceptibility and heat capacity measurements. We also discuss a possible structural mechanism for the transformation.

Introduction

Structural transformations are a very fertile research area where physicochemical, ceramic, and earth sciences overlap to investigate basic aspects of the materials and possible applications. In this sense, besides the numerous applications of, for example, spinel-like magnetic ferrites,[1] the spinel structure is also important to both material sciences and geosciences. For instance, the discontinuities at 410 and 660 km in the earth's mantle are associated with spinel transformations: the first an olivine to spinel transition, a "simple" change in stacking that could be relevant to earthquakes; the second a spinel to perovskite plus ferropericlase (magnesiowüstite) decomposition.[2]

In laboratory experiments under pressure, the AB_2X_4 spinel undergoes interesting phase transformations to the $CaFe_2O_4$-type (CF) and $CaTi_2O_4$-type (CT) structures.[3] This process, which has also been discovered naturally, as it was first observed in the Suizhou meteorite,[4] has been reproduced over a large number of oxides; e.g., $MgAl_2O_4$, $MgCr_2O_4$, $ZnCr_2O_4$, $ZnFe_2O_4$, $CoFe_2O_4$, $LiMn_2O_4$, and $CuRh_2O_4$ have been found to present this spinel-CF-type transformation under pressure and temperature.[5−11] It is interesting to note that one of the qualitative limiting criteria for the CF-type structure to appear is the ratio r_B/r_A, where r_B and r_A are the B and A ionic radii, respectively. No CF oxide with $r_B/r_A < 0.53$ has ever been found.[12] On the other hand, CT-type structure compounds have been less investigated mainly because of their difficult syntheses.[13] They require substantially higher pressures!

$CdCr_2O_4$ crystallizes in the cubic spinel structure, similar to $MgCr_2O_4$ and $ZnCr_2O_4$.[14] Other chromites(III) crystallize either in a $SrCr_2O_4$-type structure (like $SrCr_2O_4$ itself, $BaCr_2O_4$, or α-$CaCr_2O_4$[15]) or in the $CaFe_2O_4$-type structure (such as the β-$CaCr_2O_4$ polymorph[16]). In each of these compounds, the [Cr−O_6] octahedra are connected in different ways, and this contributes to the differences in their physical properties. For instance, the $CdCr_2O_4$ magnetism is quite complex, with a spiral spin structure.[17] Taking into account that, in $CdCr_2O_4$,

*To whom correspondence should be addressed. E-mail: gozdriov@gmail.com.

(1) Sun, S.; Zeng, H. *J. Am. Chem. Soc.* **2002**, *124*, 8204.
(2) Helffrich, G. R.; Wood, B. J. *Nature* **2001**, *412*, 501.
(3) Chen, M.; Shu, J.; Mao, H.; Xie, X.; Hemley, R. *Proc. Natl. Acad. Sci. U.S.A.* **2003**, *100*, 14651.
(4) Chen, M.; Shu, J.; Xie, X.; Mao, H. K. *Geochim. Cosmochim. Acta* **2003**, *67*, 3937.
(5) Irifune, T.; Fujino, K.; Ohtani, E. *Nature* **1991**, *349*, 409.
(6) Wang, Z.; O'Neill, H. S. C.; Lazor, P.; Saxena, S. K. *J. Phys. Chem. Solids* **2002**, *63*, 2057.
(7) Wang, Z.; Lazor, P.; Saxena, S. K.; Artioli, G. *J. Solid State Chem.* **2002**, *165*, 165.
(8) Wang, Z.; Schiferl, D.; Zhao, Y.; O'Neill, H. S. C. *J. Phys. Chem. Solids* **2003**, *64*, 2517.
(9) Wang, Z.; et al. *Phys. Rev. B* **2003**, *68*, 094101.
(10) Yamaura, K.; et al. *J. Am. Chem. Soc.* **2006**, *128*, 9448.
(11) Ohgushi, K.; Gotou, H.; Yagi, T.; Ueda, Y. *J. Phys. Soc. Jpn.* **2006**, *75*, 023707.
(12) Müller-Buschbaum, Hk. *J. Alloys Compd.* **2003**, *349*, 49.
(13) Geselbracht, M. J.; et al. *J. Solid State Chem.* **2006**, *179*, 3489.
(14) Verwey, E. J. W.; Heilmann, E. L. *J. Chem. Phys.* **1947**, *15*, 174.
(15) Pausch, H.; Müller-Buschbaum, Hk. *Z. Anorg. Allg. Chem.* **1974**, *405*, 1.
(16) Hill, P. M.; Peiser, H. S.; Rait, J. R. *Acta Crystallogr.* **1956**, *9*, 981.
(17) Matsuda, M.; et al. *Phys. Rev. B* **2007**, *75*, 104415.

Published on Web 02/15/2010

$r_{Cr}/r_{Cd} \approx 0.56$, this compound is likely to crystallize in the CF-type structure under the appropriate conditions.

Motivated by these facts, we have synthesized a new $CdCr_2O_4$ polymorph that crystallizes in the CF-type structure (henceforth, β-$CdCr_2O_4$). The spinel structure itself is likely to be magnetically frustrated, meaning that the system is unable to satisfy competing interactions, giving rise to largely degenerated ground states. When a spinel transforms to the CF-type structure, the [Cd−O_4] connecting tetrahedra widen to form a bicapped trigonal environment. This, along with the existence of both edge- and corner-sharing [Cr−O_6] octahedra in the CF-type structure, suggests that direct cation−cation interactions may compete against cation−anion−cation ones and could also originate interesting physicochemical properties such as superconductivity, low dimensionality, and strongly correlated features.[18]

In this article, we report the synthesis and structural and magnetic characterization of a novel β-$CdCr_2O_4$ polymorph synthesized under high-pressure and high-temperature conditions. Moreover, a structural mechanism is proposed for the first time to describe the high-pressure transformation of $CdCr_2O_4$ from the spinel polymorph to the CF-type structure.

Experimental Section

β-$CdCr_2O_4$ was prepared in a two-step process: (1) The cubic spinel was prepared by firing stoichiometric amounts of CdO and Cr_2O_3 at 1000 °C for 3 days at room pressure. (2) The obtained compound was placed within a platinum capsule and treated at 10 GPa and 1100 °C for 6 h in a multianvil press located at the Bayerisches Geoinstituit.

The crystal structure was studied with conventional powder X-ray diffraction (XRD) on an X'Pert PRO ALPHA 1 (Panalytical) instrument with a germanium monochromator (Cu $K\alpha_1$ = 1.54056 Å). XRD data were collected with a step of 0.017° from $2\theta = 10°$ to 110° over a period of 12 h. Structural refinements were undertaken using the Rietveld program *Fullprof*.[19] For transmission electron microscopy (TEM), the samples were prepared by grinding the powder, dispersing it in *n*-butyl alcohol, and collecting a few drops of the suspension on a holey carbon-coated copper grid. For the microstructural characterization, selected area electron diffraction (SAED) was performed on a JEOL JEM FX2000 microscope equipped with a double-tilt ±45° holder, working at 200 keV. High-resolution TEM (HRTEM) was carried out on a JEOL JEM 3000FEG microscope, with C_S = 0.6 nm, operating at 300 keV. HRTEM multislice image simulations were carried out using the *EMS* suite of programs.[20] The composition was checked in situ with a Link Pentafet model 5947 Oxford Microanalysis Group X-ray spectrometer coupled to the microscope. For the electron energy loss spectra (EELS), we used an ENFINA EELS system placed in the 300 keV microscope, operating in the diffraction mode with a collection semiangle of 8.9 mrad and a dispersion of 0.2 eV/channel. Magnetic susceptibility measurements were performed over the temperature range 2−300 K using a Squid Quantum Design XL-MPMS magnetometer under zero-field-cooling (ZFC) and field-cooling (FC) conditions. Specific heat and resistivity measurements were performed using a Quantum Design PPMS. However, for this resistivity measurement, the insulating behavior of the material at room temperature prevented us from obtaining a reliable measurement with our device.

(18) Tokura, Y.; Nagaosa, N. *Science* **2000**, *288*, 462.
(19) Rodríguez-Carvajal, J. *Physica B* **1993**, *192*, 55.
(20) Stadelmann, P. *JEMS*, version 20105.

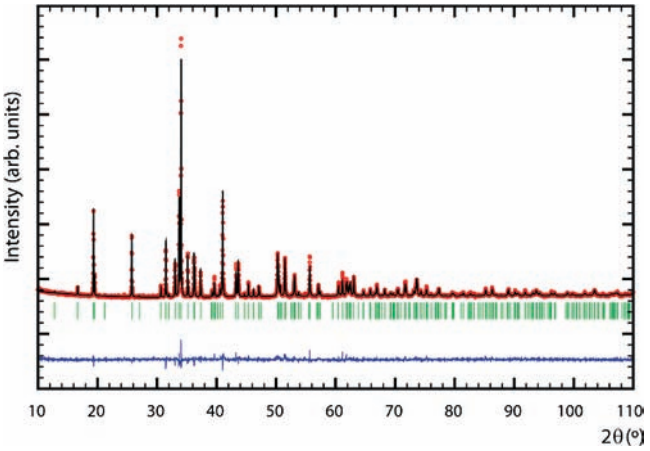

Figure 1. Rietveld refinement of the XRD pattern for β-$CdCr_2O_4$: experimental spectrum (dots), calculated pattern (continuous line), difference (bottom line), and Bragg positions (vertical lines).

Table 1. Atomic Coordinates, Isotropic Displacements, and Crystallographic Data of β-$CdCr_2O_4$[a]

atom	site	fraction	*x*	*y*	*z*	*B* (Å^2)
Cd	4c	0.950(2)	0.7593(2)	0.6596(1)	1/4	0.21(2)
Cr1	4c	0.988(2)	0.4140(3)	0.1007(3)	1/4	0.34(7)
Cr2	4c	0.982(2)	0.4413(3)	0.6155(3)	1/4	0.26(7)
O1	4c	1[b]	0.2068(9)	0.1575(8)	1/4	0.4[b]
O2	4c	1[b]	0.1195(9)	0.4829(9)	1/4	0.4[b]
O3	4c	1[b]	0.5296(12)	0.7868(9)	1/4	0.4[b]
O4	4c	1[b]	0.4188(9)	0.4329(8)	1/4	0.4[b]

[a] Space group *Pnam*, a = 9.0868(1) Å, b = 10.6242(1) Å, c = 2.9453(1) Å, Z = 4, V = 284.345 Å^3, R_p = 4.44%, R_{wp} = 5.70%, R_{exp} = 4.64%, and χ^2 = 1.51. [b] Fixed in the refinement.

Results

Synthesis, Structure, and Microstructure. The spinel-type $CdCr_2O_4$ compound fully transforms into β-$CdCr_2O_4$ at 10 GPa and 1100 °C with no signature of any remaining spinel in the final product, as indicated by the refinement of the powder XRD data. Room temperature XRD data of β-$CdCr_2O_4$ (Figure 1) were consistent with the high-pressure postspinel polymorph with the $CaFe_2O_4$-type structure.[16] The lattice parameters were measured to be a = 9.0868(1) Å, b = 10.6242(1) Å, and c = 2.9453(1) Å in the space group *Pnam*. The structural parameters, crystallographic data, and selected bond distances and angles are listed in Tables 1 and 2. Figure 2a shows a schematic view of the structure of β-$CdCr_2O_4$. The Cr ions occupy two different crystallographic sites (Cr1 and Cr2), both of them octahedrally coordinated with O ions. Each of these octahedra form alternating "double rutile chains" along the *c* axis (Figure 2b), and the oxygen coordination environments for Cr1 and Cr2 atoms are slightly different from one another. Details of the local structure around the Cr and Cd ions, as obtained from the average structural refinement, are outlined in Figure 2c,d. The mean bond ⟨Cr−O⟩ distances are 1.981(42) and 2.008(37) Å for Cr1 and Cr2, respectively (see Table 2).

In order to search for partial transformations, i.e., the coexistence of spinel and $CaFe_2O_4$ types, we checked the sample in the electron microscope but found no indication of this occurrence, implying a complete transition. Figure 3a shows SAED patterns along the [010], [011],

Table 2. Selected Bond Distances and Angles in the Structure β-$CdCr_2O_4$

atom		distances (Å) ± 0.001	atoms	angles (deg) ± 0.01
Cd	O1 × 2	2.458	Cr1−O1−Cr1	97.6
	O2 × 2	2.382	Cr1−O1−Cr1	97.7
	O3	2.487	Cr1−O2−Cr1	97.7
	O3	2.521	Cr1−O3−Cr1	97.1
	O4 × 2	2.399	Cr1−O1−Cr2	124.1
	mean	2.436(52)	Cr1−O3−Cr2	131.4
Cr1	O1	1.978	Cr2−O1−Cr2	92.2
	O2	2.067	Cr2−O4−Cr2	100.8
	O2 × 2	1.956	Cr2−O4−Cr2	94.1
	O3 × 2	1.965	O1−Cr1−O2	172.3
	mean	1.981(42)	O2−Cr1−O3	173.7
Cr2	O1 × 2	2.044	O1−Cr2−O4	177.3
	O3	1.989	O3−Cr2−O4	162.2
	O4	1.945		±0.001
	O4 × 2	2.012	Cr1−Cr1 dirutile	3.031
	mean	2.008(37)	Cr1−Cr1 along the chain	2.945
Δd(Cr1)[a]		3.893	Cr2−Cr2 dirutile	3.054
Δd(Cr2)[a]		2.874	Cr2−Cr2 along the chain	2.945

[a] $\Delta d = (1/N)\sum[(d_i^2 - \langle d\rangle)/\langle d\rangle]^2 \times 10^4$.

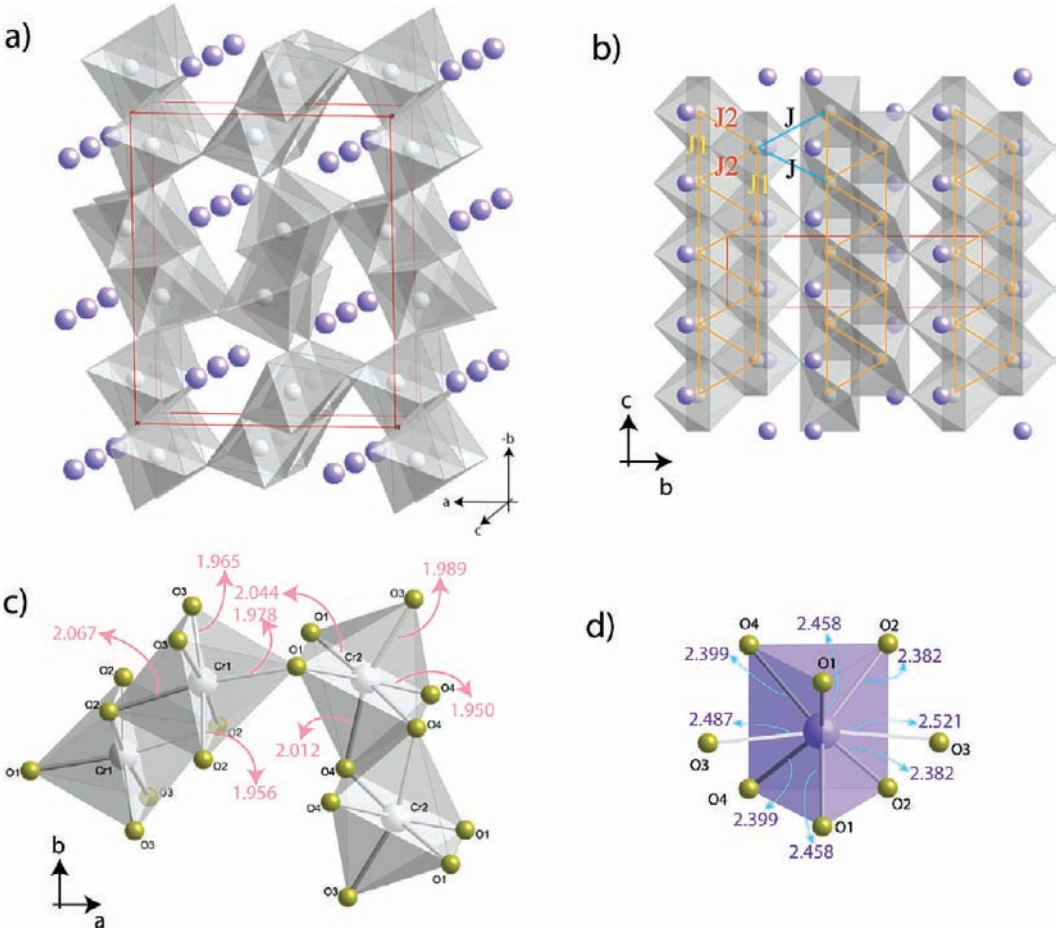

Figure 2. (a) Schematic crystal structure of β-$CdCr_2O_4$. (b) Viewed along the *a* axis, showing the three different exchange interactions (see the text). (c) ⟨Cr−O⟩ distances in both ladders. (d) Bicapped trigonal environment around Cd.

and [021] zone axes. These diagrams are in good agreement with the simulation of the diffraction patterns with the obtained X-ray cell (Figure 3b). Extra reflections appearing in the experimental patterns are due to the double diffraction originating from the encircled reflections indicated in Figure 3b. The HRTEM images along the [100] and [010] zone axes display a well-ordered structure free from defects, and the simulated image matches well to the corresponding crystal structure (Figure 4).

Energy-dispersive spectroscopic analysis performed in numerous crystallites also confirms a cationic ratio of 1:2 Cd/Cr, which agrees with the expected stoichiometry. EELS spectra collected on both β-$CdCr_2O_4$ and the isostructural β-$CaCr_2O_4$ are shown in Figure 5. Both compounds show almost identical Cr L-edges and slight

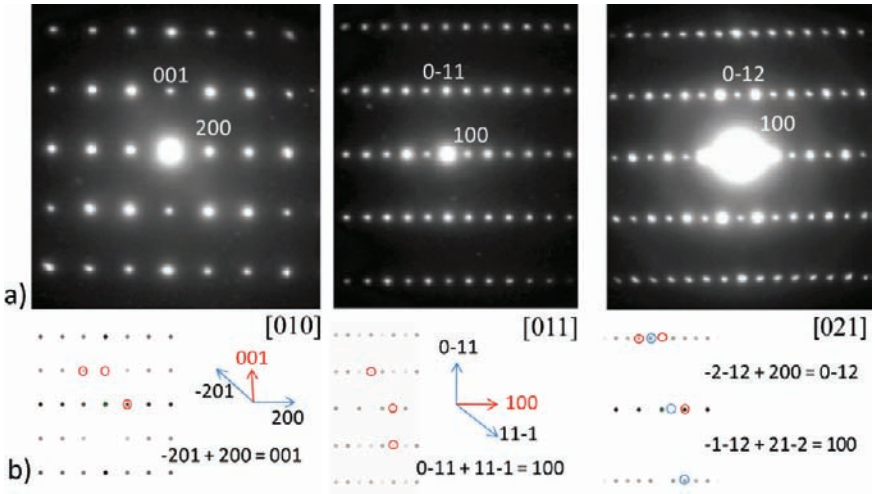

Figure 3. (a) SAED patterns for β-$CdCr_2O_4$ along the [010], [011], and [021] zone axes. (b) Calculated SAED patterns that show the cause of the double diffraction into the micrographs.

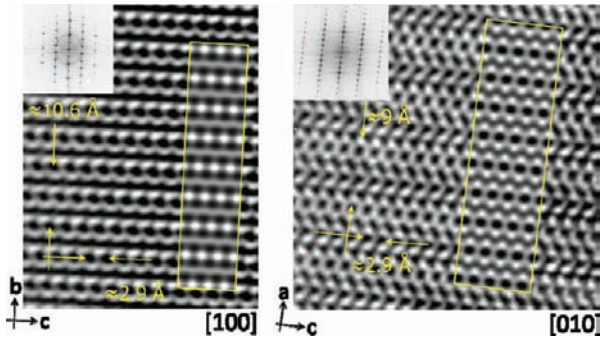

Figure 4. HRTEM images along the [100] and [010] zone axes accompanied by their fast Fourier transform and simulated images with the β-$CdCr_2O_4$ refined structure taken as the model.

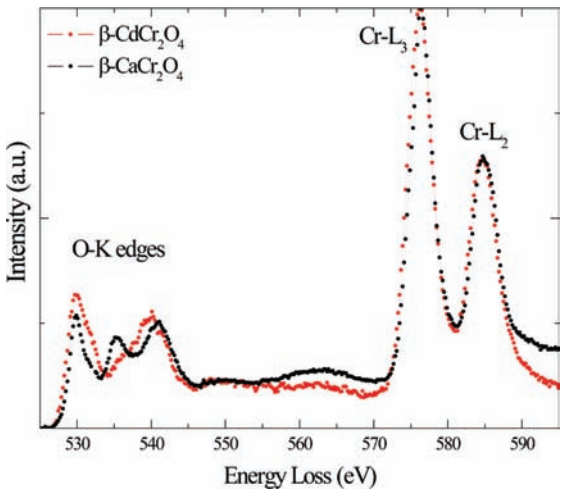

Figure 5. EELS spectra for β-$CdCr_2O_4$ and β-$CaCr_2O_4$ showing O K-edges and Cr L-edges. The spectra are aligned and normalized to the Cr L_3 maximum; the great difference in the O K-edges is evident.

differences in the O K-edges. The origin of those differences can be determined by a direct comparison with their density of states,[21] and we can conclude that those differences arise primarily from the different Cd−O and Ca−O interactions (see the Supporting Information). The difference in energy between the O K-edges and Cr

(21) Arévalo-López, A. M.; Castillo-Martínez, E.; Alario-Franco, M. A. *J. Phys.: Condens. Matter*. **2008**, *20*, 505207.

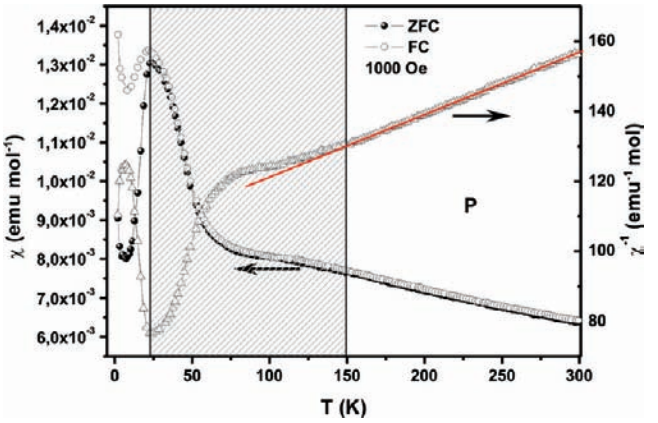

Figure 6. Temperature dependence of the susceptibility and its reciprocal of β-$CdCr_2O_4$. From 300 to 150 K, the compound behaves as a paramagnet (zone P). From 150 to ~25 K, there is low-dimensionality ordering (shaded region). Complex noncollinear AFM ordering is present below ~25 K.

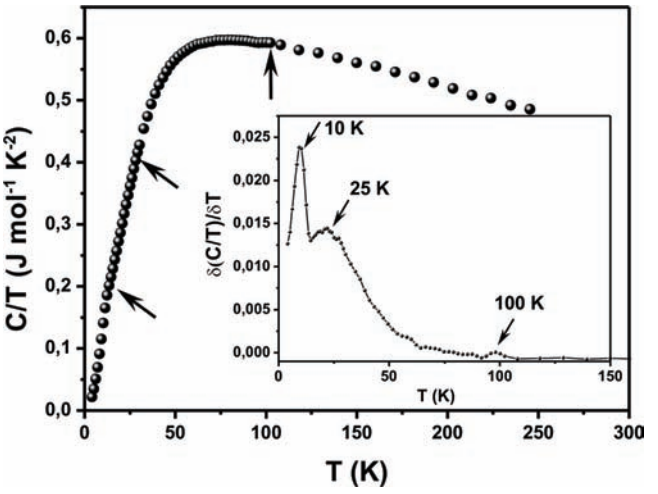

Figure 7. C_p/T vs T measurement for β-$CdCr_2O_4$. Inset: first derivative with the three different transitions marked by arrows (see the text).

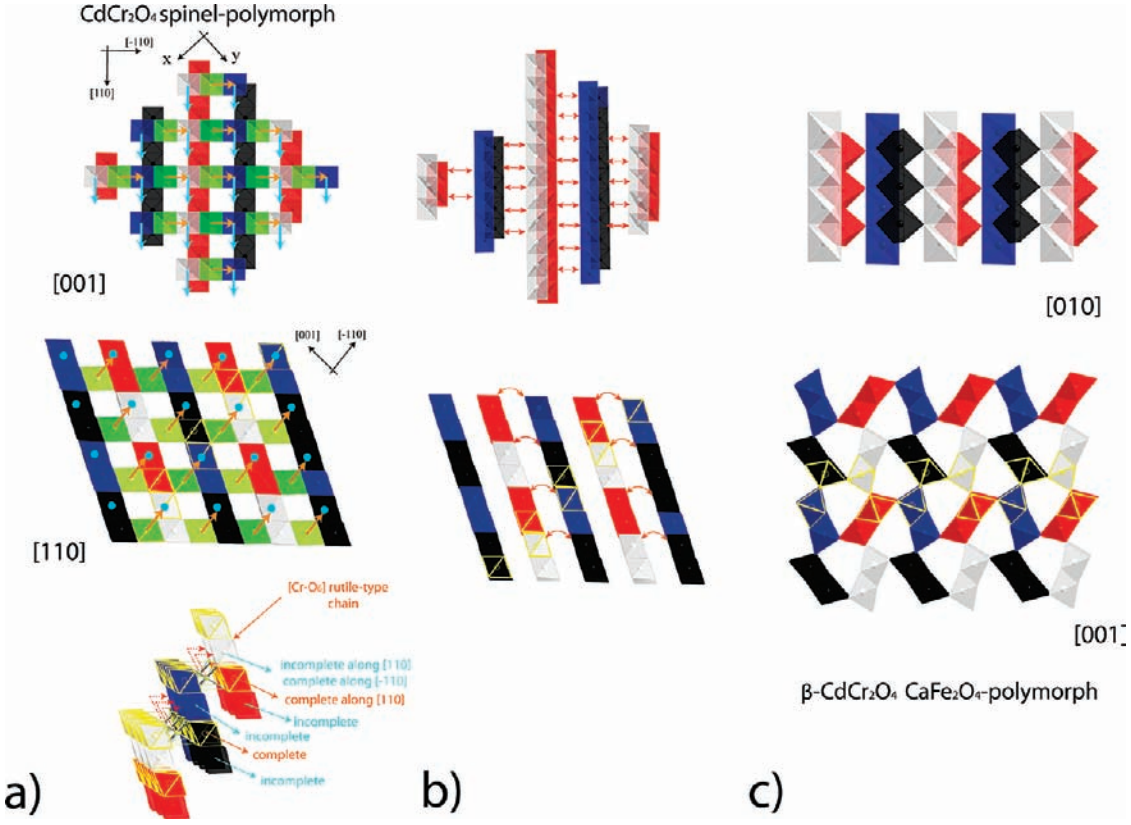

Figure 8. Spinel to CF-type transformation. (a) Spinel $[(Cr_2)O_4]$ framework viewed along the [001] (top) and [110] (middle) directions and details of the chromium displacements necessary to achieve the double rutile-like edge-sharing octahedral chains characteristic of the CF-type structure (bottom). Arrows indicate the direction of Cr ion jumps. (b) Intermediate step between the spinel and CF-type structure. A formal shear operation every other double chain, schematized by red arrows, led to the octahedral environment of the CF-type. (c) β-$CdCr_2O_4$ structure viewed along the [010] and [001] directions.

L-edges and the value of the average ⟨Cr−O⟩ distance indicate a Cr^{3+} oxidation state.[22]

Magnetic Properties. Figure 6 shows the temperature dependence of both the magnetic susceptibility and its reciprocal for β-$CdCr_2O_4$ from 300 to 2 K measured in the ZFC and FC modes at 1000 Oe. From the corresponding reciprocal susceptibility plot, the experimental magnetic moment obtained is 3.4 μ_B/Cr ion, which agrees with the theoretical $S = {}^3/_2$ Cr^{3+} (3.87 μ_B). Taking the negative Weiss temperature, $\theta_{CW} \approx -592$ K, into account, it is reasonable to expect frustrated antiferromagnetic (AFM) interactions. Upon cooling below 150 K, the susceptibility deviates increasingly from Curie−Weiss behavior, with a broad maximum centered at about 100 K, indicative of low dimensionality in the spin system. This broad maximum is also observed in the alternating-current (AC) susceptibility data (see the Supporting Information for further details). Then, the susceptibility increases abruptly up to ~25 K, this is followed by a pronounced drop typical of AFM correlations, and finally another anomaly is apparent at 10 K. The upturn at low temperatures can be ascribed to the presence of some paramagnetic impurities or even to the magnetic chain terminations that are observed in some related low-dimensional systems.[23] These magnetic transitions are confirmed by specific heat data. The C_p/T vs T plot depicted in Figure 7 shows a small jump at 100 K and consecutive slope changes at 25 and 10 K. These three magnetic transitions are more visible in the first derivative of C_p/T vs T data (inset of Figure 7). The fact that successive magnetic transitions are seen in a narrow interval of temperature is indicative of noncollinear complex magnetic structures. For instance, β-$CaCr_2O_4$ (also displaying the CF-type structure!) and β-MnO_2, a rutile-type compounds also have this characteristic and appear to have a screw-type order at low temperatures.[24,25]

Discussion

Mechanism for the High-Pressure Transformation. Despite the fact that other oxides have been found to display this high pressure-induced transition, a mechanism for this transformation has never been established. Here we propose a possible mechanism for the high-pressure transformation from the spinel to the CF structure that is depicted in Figure 8.

The spinel structure consists of a cubic close-packed array of anions, O anions in this case, in which ${}^1/_8$ of the tetrahedral and ${}^1/_2$ of the octahedral interstices are occupied by Cd and Cr cations, respectively.[14] Figure 8a only shows, for clarity, the octahedral framework of the spinel structure along the planes [001] and [110] without the Cd atoms: this is, incidentally, equivalent to the Atacamite structure.[26] It consists of two arrays of perpendicularly

(22) Arévalo-López, A. M.; Alario-Franco, M. A. *Inorg. Chem.* **2009**, *48*, 11843.
(23) Moreira-DosSantos, A.; et al. *Phys. Rev. B* **2005**, *72*, 092403.
(24) Damay, F. et al. arXiv:0906.3378.
(25) Yoshimori, A. *J. Phys. Soc. Jpn.* **1959**, *14*, 807.
(26) Wells, A. F. *Structural Inorganic Chemistry*; Clarendon Press: Oxford, U.K., 1975.

crossing [Cr−O_6] edge-sharing octahedra forming rutile-like chains running along [110] and [−110] alternating along the *c* axis (Figure 8a).

On the other hand, the CF-type structure contains double rutile-like edge-sharing chains. So, in order to get these double chains from the spinel, along say [110], we have to displace alternatively every other metal M from the second [−110] chain, vector ($^1/_4$, $^1/_4$, 0) along [110] (blue arrows), and the other metal M, vector ($-^1/_4$, $^1/_4$, 0) along [−110] (orange arrows), as inferred from Figure 8a. In this way, an M cation goes from one octahedral site to the next just by edge-crossing. These displacements complete the double rutile-like edge-sharing octahedral chains along [110] (see Figure 8b). The last step is simply a "cylindrical shear" type of operation, similar to the classic example of ReO_3 described by Hyde and O'Keeffe (see Figure 4 in ref 27), thus giving the CF-type structure (Figure 8c).

It is worth pointing out that both the second and final steps of our proposed mechanisms require not only simple cation displacements, as in our first step, but also a full octahedral movement, which implies a reconstructive transformation. This is the likely reason why we need high temperature and high pressure to force the highly stable spinel structure to be converted into the $CaFe_2O_4$ one. Obviously, the fact that only $^1/_8$ of the tetrahedral sites are occupied by cadmium simplifies the operation.

Besides, the Cd atoms that are localized in the tetrahedral sites of the $CdCr_2O_4$ spinel shift from the center of gravity toward the empty tetrahedra, which results in an environment in which the Cd atom is surrounded by eight O atoms, forming a bicapped trigonal prism at an average ⟨Cd−O⟩ distance of 2.436(52) Å (Figure 2d). All of these changes generate an increase in the density of 10.6%, which is comparable with similar transformations; for instance, there is a 9.4% increase in the density in the iron−chromite spinel−CF transformation [3], with the Cd ion being a heavier ion than the Fe one.

Magnetism. In β-$CdCr_2O_4$, only the Cr^{3+} ($S = ^3/_2$) ions are magnetic, and as described in the previous structural analysis, two sets of crystallographically inequivalent Cr atoms (Cr1 and Cr2), arranged in edge-sharing octahedra, build double rutile chains along the *c* axis, with the Cd ions situated in the tunnels between the chains. Interconnection between two double rutile chains is effective through [Cr1−O_6] octahedra within a chain-sharing corner with the [Cr2−O_6] octahedra in the adjacent chain. It is quite important to remark that the double rutile chains form a zigzag ladder, which can result in geometrical frustration if interactions (J_1⟨Cr−Cr along the *c* direction⟩ and J_2⟨Cr−Cr double rutile⟩) are comparable. This could be the case because the distances along and into the chain only differ by 0.086(2) and 0.109(2) Å for Cr1 and Cr2, respectively. From this brief structural analysis, one can extract two useful observations: (i) intrachain interactions are cation−cation and (ii) interchain interactions are cation−anion−cation. Therefore, two mechanisms compete against each other, and magnetic order will be governed by their relative magnitudes and the sign of the spin−spin interactions.

Thus, on the one hand, we have cation−anion−cation interactions, which occur between neighboring cations whose anion octahedra share a common corner and are optimal if the cation−anion−cation angle is 180° or as small as 120°.[28] In this case, the angles are 124.1(1)° and 131.4(1)° for Cr1−O1−Cr2 and Cr1−O3−Cr2, respectively; therefore, magnetic coupling between the double rutile chains will originate strong magnetic interactions that appear to be AFM ($\theta_{CW} \approx -592$ K).

On the other hand, the cation−cation interactions may become significant if octahedral site cations have an outer-electron configuration $3d^n$ with $n \leq 5$ and the occupied octahedra share a common face or a common edge.[29] In fact, in β-$CdCr_2O_4$, Cr1 and Cr2 atoms are arranged in an edge-shared octahedral environment and Cr^{3+} has half-filled t_{2g} orbitals directed toward the octahedral edges. The absence of e_g electrons suggests that Cr−Cr interactions may be, at least, as strong as cation−anion−cation interactions. Therefore, taking into account the electronic configuration of the cations, the arrangement of the occupied octahedra into chains, and the short interatomic Cr−Cr distances, the nature of the Cr−Cr coupling is expected to be also AFM.

The experimental susceptibility measurement supports these arguments. At temperatures as high as ∼150 K, the change in the slope of the inverse susceptibility plot indicates the beginning of magnetic interactions (Figure 6). The nature of these interactions can be ascribed to low-dimensional AFM ordering, characterized by a broad maximum in both AC and direct-current susceptibility and corroborated by the small peak observed at 100 K in specific heat measurements (this low-dimensional AFM ordering arises from Cr1−O−Cr2 superexchange interactions between the chains; see below).

Cooling further, two consecutive maxima are observed at ∼25 and ∼10 K, again in both susceptibility and specific heat measurements (Figures 6 and 7, respectively), corresponding to a complex AFM ordering. As was pointed out above, the existence of consecutive magnetic transitions in a small temperature range is an indication of the presence of noncollinear complex magnetic structures.[24,25] A plausible explanation for this low-temperature ordering resides in the Cr−Cr interactions existing in the double rutile chains, which form a zigzag ladder and result in a geometrical frustration environment. A clear indication of this frustration is that $T_N \ll \theta_{CW}$ ($f = \theta_{CW}/T_N > 5$[30]). Moreover, one can see in Table 2 that inner Cr−Cr distances along and into the same double chain are quite similar, and this, therefore, suggests that nearest-neighbor J_{NN} (J_1 and J_2 in Figure 2b) magnetic interactions are comparable, originating this strong frustration.

In comparison with the β-$CaCr_2O_4$ compound (which presents a low-dimensional magnetic ordering of the Cr^{3+} spins at 24 K $< T <$ 270 K and a complex AFM ordering evidenced below $T_N = 21$ K[24]), the β-$CdCr_2O_4$ displays similar low dimensionality at high temperature (25 K $< T <$ 150 K) and again a complex AFM magnetic behavior at lower temperature (see Figure 6). Furthermore, angles and distances are comparable between both compounds

(27) Hyde, B. G.; O'Keeffe, M. *Acta Crystallogr.* **1973**, A29,243.

(28) Goodenough, J. B. *Magnetism and the Chemical Bond*; John Wiley & Sons Inc.: New York, 1963,

(29) Goodenough, J. B. *Phys. Rev.* **1960**, *117*, 1442.

(30) Greedan, J. E. *J. Mater. Chem.* **2001**, *11*, 37.

because $^{VIII}Ca^{2+}$ and $^{VIII}Cd^{2+}$ ionic radii (1.12 and 1.10 Å, respectively [31]) are very close. Yet, in spite of the structural similarities between both compounds, differences in their Curie−Weiss temperatures exist ($\theta_{CW} \approx -592$ and -270 K for β-$CdCr_2O_4$ and β-$CaCr_2O_4$, respectively) and, obviously, differences between their magnetic interactions. One way to compare these differences is by considering, in the mean-field limit, the change of J_{NN} interactions from $J = -3k_B\theta_{CW}/2zS(S+1)$, where z is the number of nearest-neighbor interactions, i.e., Cr−Cr interactions.[28] These differences are clearly noticed in their corresponding susceptibility plots. Moreover, because the compounds are isostructural, the relationship between the θ_{CW} of both compounds gives us a direct relation of the J_{NN} between them, i.e., $2.2J_{NN\text{-}\beta Ca} = J_{NN\text{-}\beta Cd}$, thus implying that the NN interactions for β-$CdCr_2O_4$ are stronger than the ones for β-$CaCr_2O_4$. Therefore, the low-dimensional AFM ordering at 100 K, which should arise from Cr−O−Cr interactions, is less noticeable in β-$CdCr_2O_4$. Otherwise, the Cr−O−Cr interchain interactions are dominant in the β-$CaCr_2O_4$ compound (Figure 4 of ref 24). A clear indication of the Cr−Cr interactions' strength in the β-$CdCr_2O_4$ compound, in contrast to those of β-$CaCr_2O_4$, is the observation of the low-temperature transitions in both susceptibility and specific heat temperature-dependent plots. The origin of these differences could be attributed to the small differences in the octahedral distortions because, in frustrated compounds, small changes in the NN and next-NN interactions greatly affect the resultant average magnetic structure.

As in β-$CaCr_2O_4$, neutron diffraction would be needed in order to elucidate its magnetic structure. We have actually performed powder neutron diffraction for β-$CdCr_2O_4$ (see the Supporting Information), but no refinable data could be obtained mainly because of the small amount of sample (we have to recall that the sample was obtained at high pressure) and to the large neutron absorption cross section of cadmium ($\sigma_a = 2520$ b). This precluded us from making any conclusion concerning the magnetic structure. We can consider this work as a starting point for further research on an isotopically adequate sample in a suitable diffractometer such as D20 or GEM.

(31) Shannon, R. D. *Acta. Crystallogr., Sect. A* **1976**, *32*, 751.

Conclusions

We have successfully transformed the $CdCr_2O_4$ spinel to its high-pressure β-polymorph with the $CaFe_2O_4$-type structure. We propose a novel structural transformation mechanism between the two structures. Because this β-$CdCr_2O_4$ structure includes both edge- and corner-sharing [Cr−O_6] octahedra, the competition between the magnetic exchange interactions is inherent to it and complex magnetic properties are not surprising in these types of arrangements. In the present case, the magnetic and heat capacity data of β-$CdCr_2O_4$ indicate a low-dimensional transition with a maximum centered at 100 K that demonstrates the Cr−O−Cr interactions. Two more transitions are observed at 25 and 10 K because the Cr−Cr interactions develop a complex AFM order.

Acknowledgment. High-pressure experiments were performed at the Bayerisches Geoinstitut under the EU "Research Infrastructures: Transnational Access Programme (Contract 505320 (RITA)-High Pressure). We thank Professor David Rubie and Dr. Dan Frost for their help with those experiments and valuable comments. The authors also thank Jessica Levin (UCM) for her comments and CONACYT México, UCM, CICYT (Projects MAT2004-01641 and MAT2007-64006), and Comunidad Autónoma de Madrid [MATERYENER program PRICYT S-0505/PPQ-0093 (2006)] for financial support.

Supporting Information Available: EELS spectra along with their simulation, ac susceptibility measurements, and neutron diffraction. This material is available free of charge via the Internet at http://pubs.acs.org.